

7-13-2020

Effect of Ruptures in some Cables on the Static and Dynamic Analysis of Cable-Stayed Bridges.

M. Naguib

Structural Eng. Dept., Mansoura University, Mansoura, Egypt

S. El Baglaty

Structural Eng. Dept., Mansoura University, Mansoura, Egypt

M. Shaaban

Structural Eng. Dept., Mansoura University, Mansoura, Egypt

Follow this and additional works at: <https://mej.researchcommons.org/home>

Recommended Citation

Naguib, M.; El Baglaty, S.; and Shaaban, M. (2020) "Effect of Ruptures in some Cables on the Static and Dynamic Analysis of Cable-Stayed Bridges.," *Mansoura Engineering Journal*: Vol. 39 : Iss. 3 , Article 6. Available at: <https://doi.org/10.21608/bfemu.2020.102685>

This Original Study is brought to you for free and open access by Mansoura Engineering Journal. It has been accepted for inclusion in Mansoura Engineering Journal by an authorized editor of Mansoura Engineering Journal. For more information, please contact mej@mans.edu.eg.

Effect of Ruptures in Some Cables on the Static and Dynamic Analysis of Cable-Stayed Bridges

تأثير تهتك بعض الكابلات على التحليل الإستاتيكي والديناميكي للكبارى ذات الكابلات

M. Naguib, S. El Baglaty, M. Shaaban
Structural Eng. Dept., Mansoura University, Mansoura, Egypt

المخلص

يهدف البحث إلى دراسة تأثير القطع الحادث في بعض كابلات الكبارى ذات الكابلات حيث تم إجراء هذا البحث للكبارى ذات الخمسة بحور بأطوال 140 م لكل من البحرين الخارجيين و 280 م للأبهر الداخلية وبطول إجمالى 1120 م وذلك للكبارى قيثارية الشكل وقد تم إجراء كلا من التحليل الإستاتيكي و التحليل الديناميكي لهذا الكوبرى بإستخدام طريقة تصغير طاقة الوضع بإستخدام طريقة الإنحدارات المتبادلة اخذاً فى الإعتبار الأحمال الرئيسية المتمثلة فى وزن المنشأ و كذلك الأحمال الحية ومؤثراتها حيث تم إستخدام مجموعة من البرامج بلغة الفورتران فى التحليل الإنشائى وقد تم إعدادها و تحقيقها بواسطة [1]. وقد تم إجراء التحليل الديناميكي لأكثر الكابلات تأثيراً على الكبارى عند قطعها والمستنتجة من التحليل الإستاتيكي وفى النهاية وبعد إعداد النتائج فى صور علاقات وجداول تم الوصول إلى الحالات الحرجة والتي تتمثل فى إنهيار الكابل الخارجى (الأكثر طولاً) فى البرج الأول ومن هنا تم الوصول إلى النتائج المستنتجة من البحث.

Abstract

This paper presents the study of cables rupture effect on cable-stayed bridges. The static and dynamic analysis for cable stayed bridge having five spans considering single plane of cables in harp shape is carried out. This study is concerned about bridges having five spans with 140 ms for exterior spans and 280 ms for the three interior spans. The total length of the bridge is 1120 ms. it's carried out for harp bridges. The own weight of all structural elements, and traffic load including impact are taken into account. In the both static and dynamic analysis, the energy method, based on the minimization of the total potential energy (TPE) of structural elements, via conjugate gradient technique is used. The procedure is carried out using the iterative steps to acquire the final configurations. Then, Dynamic Analysis is carried out for the most critical case to confirm the obtained results from static analysis. All prepared computer programs in FORTRAN language for this work and their verifications is written by [1]. All results showed that, the most critical case is the rupture of the outer cable (longest one). The conclusions, which have been drawn from the present work, are outlined.

Keywords

Cable Rupture, Conjugate gradient method, Cable-stayed Bridge.

1- Introduction

Cable stayed bridges are the bridges that have one or more towers from which cables support the floor beams. There are three major classes of cable stayed bridges harp, radiating and fan. In the harp bridges, the cables are nearly parallel. The Radiating is like the harp but the spacing between cables on the deck not equal the spacing on the tower. In the fan bridges, the cables are connected to the top of the towers. In the medium lengths, the harp bridge is preferred. The cable-stayed bridges are optimum for spans longer than

cantilever bridges and shorter than suspension bridges.

The Cables sustaining the cable-stayed bridge may break due to catastrophic cases, lack of maintenance over a long period of time, or excessive corrosion of the connection. It is also possible similar behavior may occur due to loosening a cable before replacing it.

Many studies on this type of bridge have been carried out in the last half-century. Fleming derived a stable function under the influence of the beam element to

modify the axial stiffness, to establish a structural analysis model of cable-stayed bridges using the finite element analysis concept [2]. Hegab analyzed the structure of a three dimensional double-cable plane cable-stayed bridge using the energy method with an incremental iteration approach, and also considering the torsion effect [3]. Nakamura Suzumura (2009) conducted experiments on corroded galvanized steel wires at different corrosion levels. He found that the mixed effects of corrosion and cyclic stresses fractured the wires. Wolff and Starossek [4] studied that the loss of cables can lead to overloading and rupture of adjacent cables. Huang et al., (2007) formulated a method to compute the tension and deformation of corrosion cable in an existing cable-stayed bridge. Wu et al., [5] studied the possibility of cable loosening in pre-stressed concrete cable-stayed bridge. Roland (2000) concluded that the reduction in strength of the cable due to deterioration increases with increase in dead load [6]. Chin-Sheng Kao Studied the effect of broken cables on cable-stayed bridges with individual cases of failure and his study is concerned for three span bridges [7].

In the present work, Energy method is used for the analysis, and it is a unifying approach to the analysis of both linear and non-linear structures by considering the determination of equilibrium as an iterative process of minimizing the total potential energy, the position of equilibrium being reached when the total potential energy is minimum [8], [9], [10], [11], and [12]. A summary with a step-by-step iterative procedure is presented.

Step-by-step static response analysis by minimization of the total potential energy

The point at which W (total potential work) is a minimum defines the equilibrium position of the loaded structure. Mathematically, the equilibrium condition in the i -direction at joint j may be expressed as: x_{ji}

$$\frac{\partial W}{\partial x_{ji}} = [g_{ji}] = 0, \quad i = 1, 2 \text{ and } 3 \quad (1)$$

Where:

x_{ji} = The displacement of joint j corresponding to a particular degree of freedom, direction i .

g_{ji} = The corresponding gradient of the energy surface.

The location of the position where W is the minimum is achieved by moving down the energy surface along descent vector v a distance S_v until W is a minimum in that direction, that is, to a point where:

$$\frac{\partial W}{\partial S} = 0 \quad (2)$$

From this point a new descent vector is calculated and the above process is repeated. The method is mathematically expressing this displacement vector at the $(k+1)$ th iteration as:

$$[X]_{k+1} = [X]_k + S_k v_k \quad (3)$$

Where:

v_k = The descent vector at the k th iteration from x_k in displacement space

S_k = the step length determining the distance along v_k to the point where W is a minimum.

Summary of the iterative procedures

The main steps in the iterative processes required to achieve structural equilibrium by minimization of total potential energy may be summarized as follows:

First, before the start of the iteration scheme

a) Calculate the tension coefficients for the pretension forces in the cable by:

$$t_{jn} = \left[\left(T_o + \frac{EA}{L_o} \right) / L_o \right]_{jn} \quad (4)$$

Where:

e = the elongation of cable elements due to applied load only;

t_{jn} = the tension coefficient of the force in member jn ;

T_o = initial force in a pin-jointed member or cable link due to pretension;

E = modulus of elasticity;

A = area of the cable element; and

L_o = the unstrained initial length of the cable link

b) The elements in the initial displacement vector $[X_o]$ are considered as zero.

c) Calculate the lengths of all the elements in the pretension structure using:

$$L_o^2 = \sum_{i=1}^3 (X_{ni} - X_{ji})^2 \quad (5)$$

Where:

X = element in displacement vector due to applied load only.

d) To meet the convergency with minimum time, the technique of scaling matrix is used [13], [14] and [15]. The elements in the scaling matrix are given by:

$$H = \text{diag}\{k_{11}^{-1/2}, k_{22}^{-1/2}, \dots, k_{nn}^{-1/2}\} \quad (6)$$

Where:

n = total number of degrees of freedom of all joint;

k = the 12 x 12 matrix of the element in global co-ordinates.

The steps in the iterative procedure then are summarized as

Step (1) Calculate the elements in the gradient vector of the TPE, using:

$$g_{ni} = \sum_{n=1}^{f_n} \sum_{r=1}^{12} (k_{nr} x_r)_n - \sum_{n=1}^{P_n} \left(t_{jn} (X_{ni} + x_{ni} - X_{ji} - x_{ji}) \right) - F_{ni} \quad (7)$$

Step (2) Calculate the Euclidean norm of the gradient vector, $R_k = [g_k^T g_k]^{1/2}$, and check if the problem has converged. If $R_k \leq R_{min}$ stop the calculations and print the results. If not proceed to step (3).

Step (3) Calculate the elements in the descent vector, v using:

$$[v]_{k+1} = -[H][g]_{k+1} + \beta_k [v]_k \quad (8)$$

$$\text{Where: } [v]_o = -[g]_o \quad (9)$$

$$\text{And } \beta_k = \frac{[g]_{k+1}^T [H]^T [H][g]_{k+1}}{[g]_k^T [H]^T [H][g]_k} = \frac{[g]_{k+1}^T [R][g]_{k+1}}{[g]_k^T [R][g]_k} \quad (10)$$

Step (4) Calculate the coefficients in the step-length polynomial form:

$$C_4 = \sum_{n=1}^P (EAa_3^2/2L_o^3)_n \quad (11a)$$

$$C_3 = \sum_{n=1}^P (EAa_2a_3/L_o^3)_n \quad (11b)$$

$$C_2 = \sum_{n=1}^P \left[t_o a_3 + \frac{EA(a_2^2 + 2a_1a_3)}{2L_o^3} \right]_n + \sum_{n=1}^f \sum_{s=1}^{12} \sum_{r=1}^{12} \left(\frac{1}{2} v_s k_{sr} v_r \right)_n \quad (11c)$$

$$C_1 = \sum_{n=1}^P \left[t_o a_2 + \frac{EAa_1a_2}{L_o^3} \right]_n + \sum_{n=1}^f \sum_{s=1}^{12} \sum_{r=1}^{12} (x_s k_{sr} v_s)_n - \sum_{n=1}^N F_n v_n \quad (11d)$$

Where:

$$a_1 = \sum_{i=1}^3 \left[(X_{ni} - X_{ji}) + \frac{1}{2} (x_{ni} - x_{ji}) \right] (x_{ni} - x_{ji}) + L_o^2 \frac{T_o}{EA} \quad (12a)$$

$$a_2 = \sum_{i=1}^3 \left[(X_{ni} - X_{ji}) + (x_{ni} - x_{ji}) \right] (v_{ni} - v_{ji}) \quad (12b)$$

$$a_3 = \sum_{i=1}^3 \frac{1}{2} (v_{ni} - v_{ji})^2 \quad (12c)$$

Where:

f = Number of flexural members;

P = Number of pin-jointed members and cable links;

F = Element in applied load vector; and

K_{sr} = Element of stiffness matrix in global co-ordinates of a flexural element.

Step (5) Calculate the step-length S using Newton's approximation formula as:

$$S_{k+1} = S_k - \frac{4C_4S^3 + 3C_3S^2 + 2C_2S + C_1}{12C_4S^2 + 6C_3S + 2C_2} \quad (13)$$

Where:

k is an iteration suffix and $S_{k=0}$ is taken as zero

Step (6) Update the tension coefficients using the following equation:

$$(t_{ab})_{k+1} = (t_{ab})_k + \frac{EA}{(L_o^3)_{ab}} (a_1 + a_2s + a_3s^2)_{ab} \quad (14)$$

Step (7) Update the displacement vector using equation (4).

Step (8) Repeat the above iteration by returning to step (1).

2- Bridge Description

With reference to Fig. (1), which shows the configuration of a five-span cable-stayed bridge. The bridge has two equal

exterior spans of 140 m, each, and the interior spans are 280 m long, each. The deck girder has a total span of 1120 m. The bridge is symmetrical and composed of three major elements: (a) the deck girder, (b) four pylons and (c) eleven cables on each side of the pylons. The cables were 6x37 classes IWRC [16] of zinc-coated bridge ropes. All cables have an area of 61.94 cm^2 , diameter of 10.16 cm, own weight of 48.96 kg/m, modulus of elasticity of 1584 t/cm^2 , and the maximum failure load of 925 tons. The initial tension in all cables was taken as 30 % of the maximum failure load (925 tons) for the 1st iteration then circle of solution technique is used with 20 cycles [1]. All section properties for cables, pylons and floor beam are given in Table (1).

3- Analysis Considerations

The static and dynamic analysis for cable-stayed bridge of harp shape with all mentioned geometry and properties is carried out. All bridge elements were analyzed as a space structure. A uniform load along the whole span is considered for the analysis of cables failure. The model considered single plane of cables with 2598 degrees of freedom with rigid connection between deck and pylon. The total equivalent live load for the girder including impact effect on the bridge is 5.28 t/m'. Individual cases of cable failure are considered, then combination ones and all are in the same case of loading to make the study more convenient.

4- Analysis of Results

Figures (3) to (39) and Table (2) showed some of the results obtained from the analysis:

1. Figs. (3) to (13) showed the comparison between vertical deflection of the deck for the most critical cases of analysis either in individual cases or combination ones. It showed that the maximum vertical deflection occurs when the outer cable is broken in the 1st pylon or in the 2nd one,

and it decreases as the broken cable is away from the outer cable. When the combination cases are carried out, the vertical deflection is more than the allowable deflection for the bridge if seven cables are broken in the same time.

2. Figs. (14) to (24) showed the comparison between bending moment for the most critical cases of analysis, it showed that the maximum bending moment increased by 147.3 % when the outer cable ruptured.

3. Figs. (25), (28) and (31) showed the comparison between the displacement of the joints at the mid-spans due to dynamic analysis.

4. Figs. (26), (29) and (32) showed the comparison between the velocity of the joints at the mid-spans due to dynamic analysis.

5. Figs. (27), (30) and (33) showed the comparison between the acceleration of the joints at the mid-spans due to dynamic analysis.

6. Figs. (25) to (39) showed the comparison between the normal force and bending moment of the joints at the mid-spans due to dynamic analysis.

7. All the dynamic results and curves confirmed the obtained results from the static analysis.

8. Table (2) represented the final tension force in all cables for each individual cable failure, and it shows that when a cable is broken the force is distributed to the surrounding cables. The distribution takes place up to two cables towards the pylon and to the first largest cable towards the center. Also the maximum final tension force in all cables reached when the outer cable is broken and don't reach the breaking load of the bridge so there is no danger on the bridge stability for these cases.

5- Major Conclusions

1. The most critical case of cables failure is when the outer cable either in the 1st pylon or in the 2nd one is broken. Therefore, when replacing these cables one must

assess the effects on the internal forces of the bridge to ensure its safety.

2. No danger on the cable stayed bridge if any of individual cable failure case occurs.

3. When a cable in a cable-stayed bridge breaks, the adjacent cables will experience a significant increase in cable forces. As such, for future replacement of the existing cable-stayed bridges, it is crucial to assess the increment of cable force that may occur in the adjacent cables in order to prevent yielding failure in the adjacent cables.

4. When the outer cable of a cable-stayed bridge breaks, the tower may undergo a significant horizontal displacement, and the center of the deck may experience significant vertical displacement. It is therefore required that a thorough assessment of the increased displacement be made in advance when replacing the outer cables.

5. From dynamic analysis, all results obtained from static analysis are approved that there is a big effect on the bridge from the outer cable rupture.

6- References

[1] Naguib, M. "Effect of Initial Sag and Initial Tension in Cables on outcome response in Cable Structure", Mansoura Engineering Journal, (MEJ), Vol.30, No.4, December 2005.

[2] Fleming, J. F., "Nonlinear static analysis of cable-stayed bridges" International Journal of Computers and Structures, Vol. 10, pp. 621-635, (1979).

[3] Hegab, H. I. A., "Energy analysis of doubled-plane cable-stayed bridges" Journal of the Structural Division, ASCE, Vol. 113, pp. 2176-2188, (1987).

[4] Wolff M., Starossed U., "Robustness Assessment of a Cable-Stayed Bridge" International conference on bridge maintenance, safety and management, Seoul, Korea, (2008).

[5] Online available: <http://www.china.org.cn/English/2002/Apr/31363.html>, (April 22,2009).

[6] Ronald M. M., "Corrosion in Suspension Bridge Cables". 16th congress of IABSE, Lucerne, (2000).

[7] Chin-Sheng K., Chang-Huan K., "The Influence of Broken Cables on The Structural Behavior of Long-Span Cable-Stayed Bridges" Journal of Marine Science and Technology, Vol. 18, No. 3, pp. 395-404, (2010).

[8] Buchholdt, H. A., "An introduction to cable roof structures", Cambridge University Press, (1985).

[9] Buchholdt, H. A., "Tension structures", Struc. Engrg., Vol. 48, No. 2, pp. 45-54.,February (1970).

[10] Buchholdt, H. A., "A nonlinear deformation theory applied to two dimensional pre-tensioned cable assemblies" Proc. Inst. Civ. Engrs., Vol. 42, pp. 129-141, (1969).

[11] Stefanou, G.D., Moossavi, E., Bishop, S., and Koliopoulos, P., "Conjugate gradients for calculating the response of large cable nets to static loads" Computers & Structures, Vol. 49, No. 5, pp. 843-848, (1993).

[12] Stefanou, G. D., and Nejad, S. E. M., "A general method for the analysis of cable assemblies with fixed and flexible elastic boundaries" Computers & Structures, Vol. 55, No.5, pp. 897-905, (1995).

[13] Bauer, F. L., "Optimally Scaled Matrices" Num. Maths., 5, 73-87, (1963).

[14] Businger, O. A., "Matrices which can be optimally scaled", Num. Maths., 12, 36-48, (1968).

[15] Fried, I., "A gradient computational procedure for the solution of large problems arising the finite element discretization method" International Journal for Numerical Methods in Engineering, 2 October-December (1970).

[16] Frederick S. Merritt, "Structural Steel Designers Handbook", Copyright by McGraw-Hill, Int., (1972).

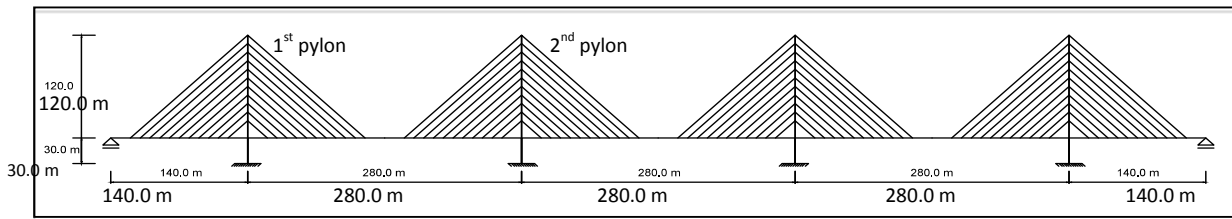


Fig. (1): Configuration of the Bridge

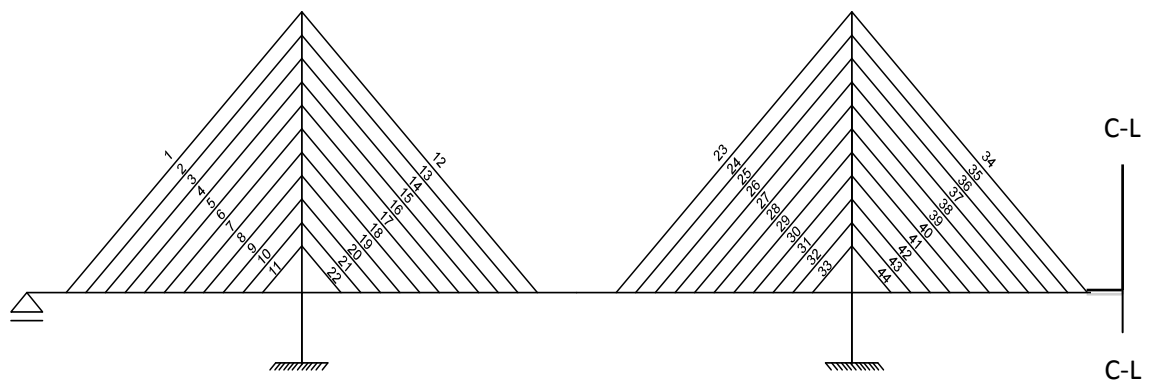


Fig. (2): Numbering of Bridge Cables

Structural Element	Description of Structural Elements	Properties of Sections					Loads	
		Moldulus of Elasticity	Area	Inertia @ X	Inertia @ Y	Inertia @ Z	Dead Load	Live Load
		t/cm ²	m ²	m ⁴	m ⁴	m ⁴	t/m	t/m
Pylon	Hollow rectangular R.C. section	300	5.76	17.66	7.4	15.9	14.4	0
Deck	Steel box girder	2100	0.625	1.14	30.5	31.64	5.78	5.28
Cables	Spiral strand	1584	0.00619354				0.04896167	0

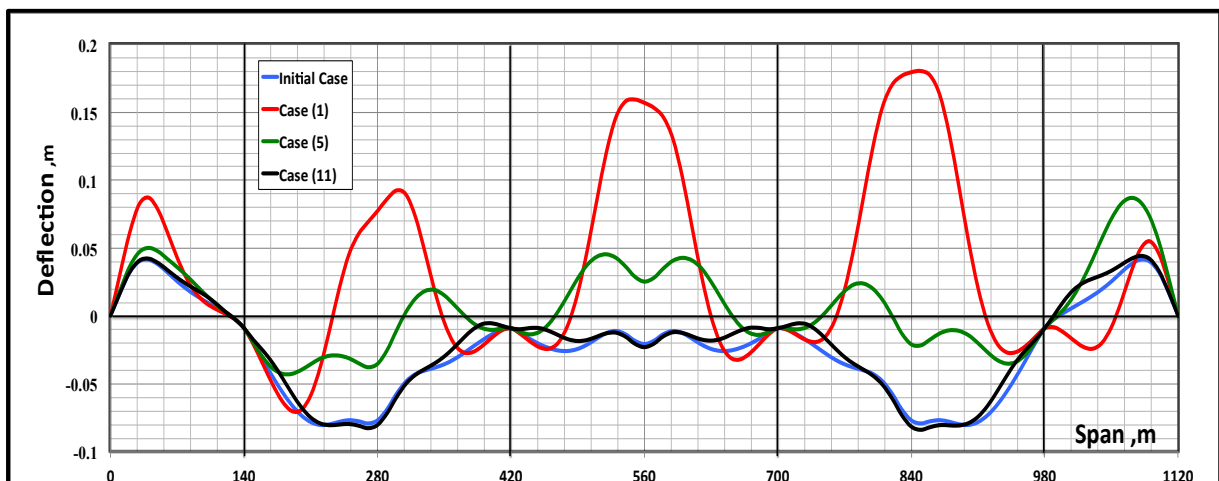
Table (1): Properties of Sections used

Cable No.	Final Tension (ton)	% Change in final tension due to cable break										
		1	2	3	4	5	6	7	8	9	10	11
1	377.981		163.44	81.09	-11.94	-37.74	-41.45	-37.77	-24.34	-5.31	10.7	20.77
2	246.458	50.42		50.2	18.9	-2.95	-11.6	-12.81	-9.15	-2.99	3.05	7.52
3	169.186	11.92	26.33		39.32	21.18	5.49	-4.26	-7.86	-6.89	-3.44	0.54
4	136.553	-1.94	8.85	29.49		43.06	24.65	6.55	-4.94	-9.54	-9.16	-6.12
5	128.706	-6.56	0.29	15	36.18		46.7	24.3	4.26	-8.17	-12.88	-13.26
6	133.376	-6.8	-3.27	4.893	18.88	39.98		47.78	22.88	1.2	-12.45	-18.88
7	145.116	-5.09	-3.89	-0.62	5.78	18.8	42.96		48.84	22.22	-1.6	-17.85
8	157.113	-2.91	-2.9	-2.6	-1.27	3.45	17.92	43.51		52.66	24.74	-1.68
9	162.978	-8.19	-1.45	-2.38	-3.41	-3.64	0.55	15.71	43.99		64.52	37.9
10	157.708	0.023	-0.232	-1.21	-2.78	-4.68	-5.92	-1.7	14.65	48.47		99.08
11	162.978	0.31	0.23	-0.25	-1.22	-2.84	-5.17	-6.07	-1.24	16.77	83.49	

Table (2): Change in final tension due to cable break (%)

Individual Cases		Combination Cases		Combination Cases	
Case	Cable No.	Case	Cable No.	Case	Cable No.
1	1	1	11	41	1,2
5	5	2	11,10	42	1,2,3
11	11	3	11,10,9	43	1,2,3,4
12	12	11	22	45	12,13
16	16	12	22,21	46	12,13,14
22	22	13	22,21,20	47	12,13,14,15
23	23	21	33,32	49	23,24
27	27	22	33,32,31	50	23,24,25
33	33	23	33,32,31,30	51	23,24,25,26
34	34	31	44,43		
38	38	32	44,43,42		
44	44	33	44,43,42,41		

Table (3): Cases of study



* Initial case: case of analysis without ruptures in cables

Fig. (3): Vertical deflection of the floor beam (individual cases)

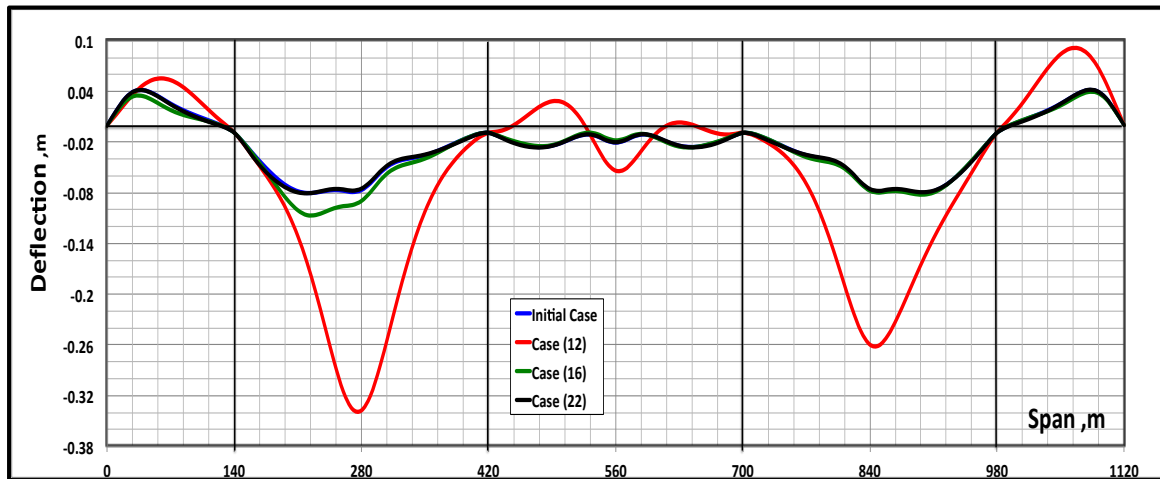


Fig. (4): Vertical deflection of the floor beam (individual cases)

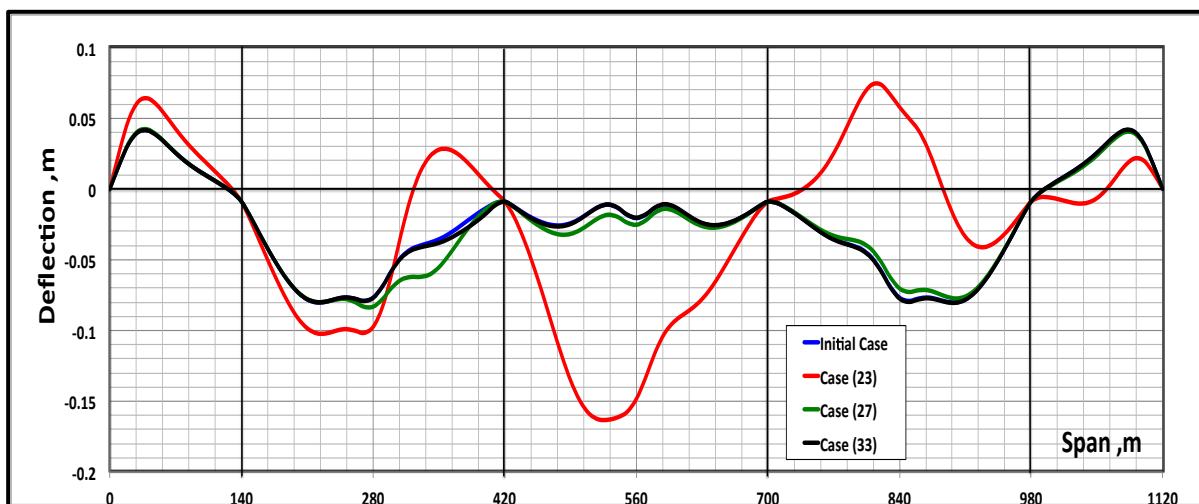


Fig. (5): Vertical deflection of the floor beam (individual cases)

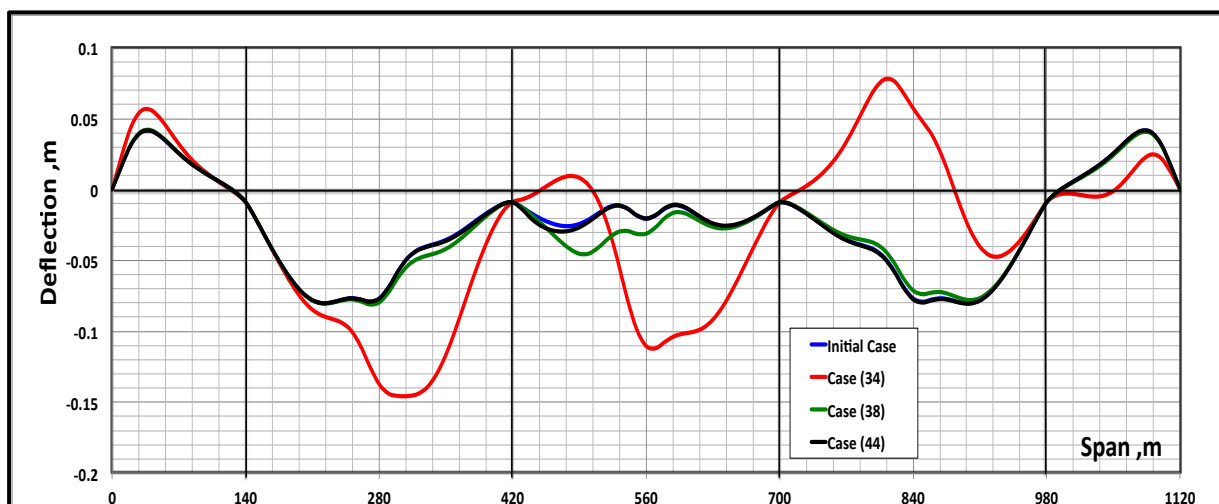


Fig. (6): Vertical deflection of the floor beam (individual cases)

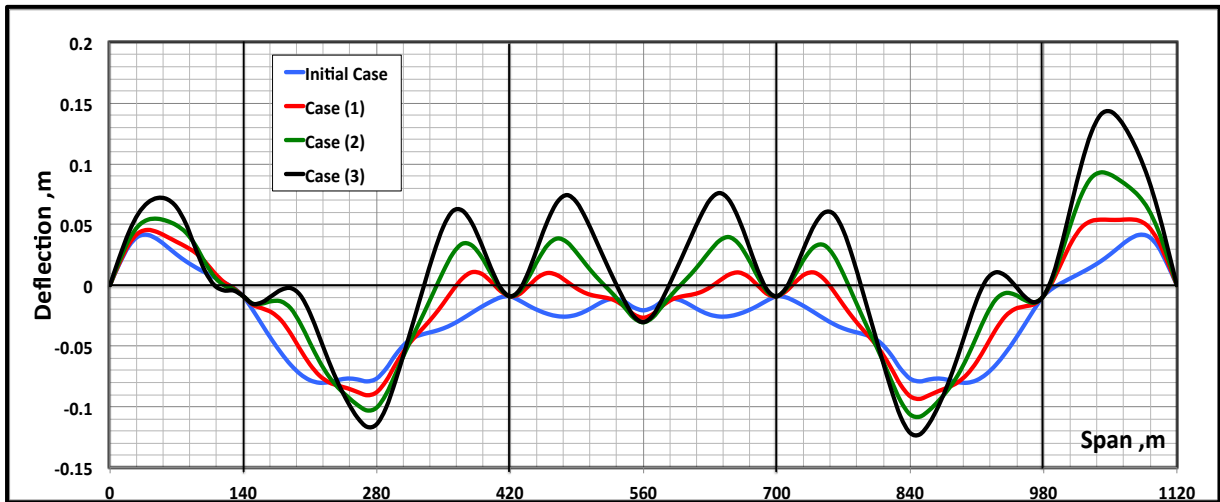


Fig. (7): Vertical deflection of the floor beam (Combination cases)

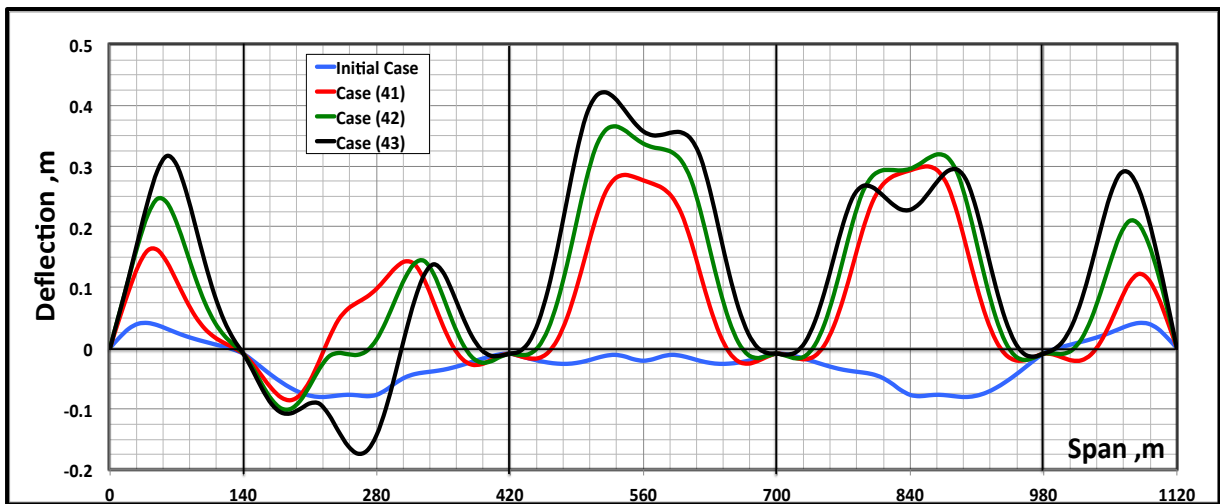


Fig. (8): Vertical deflection of the floor beam (Combination cases)

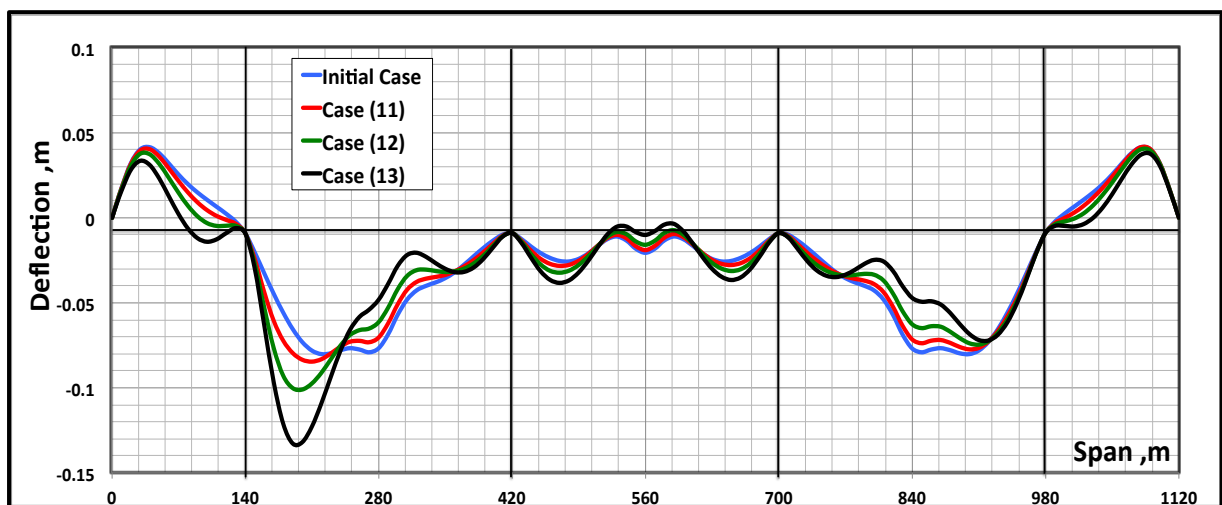


Fig. (9): Vertical deflection of the floor beam (Combination cases)

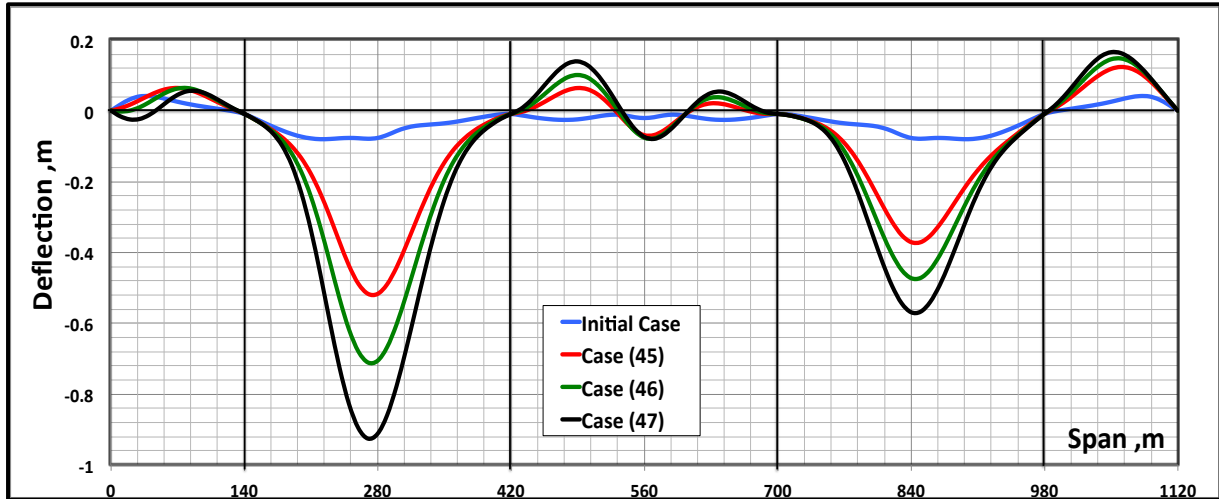


Fig. (10): Vertical deflection of the floor beam (Combination cases)

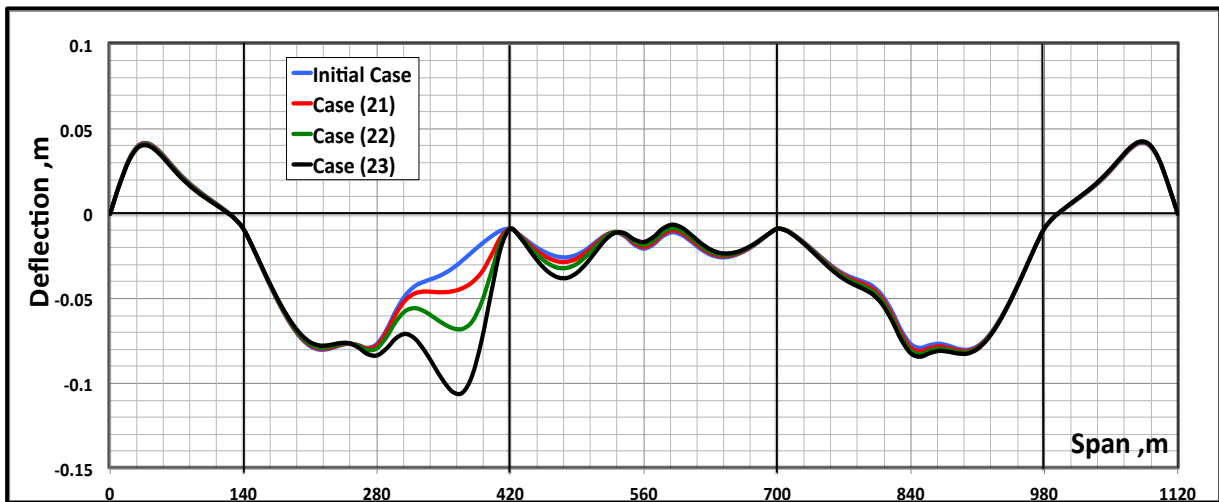


Fig. (11): Vertical deflection of the floor beam (Combination cases)

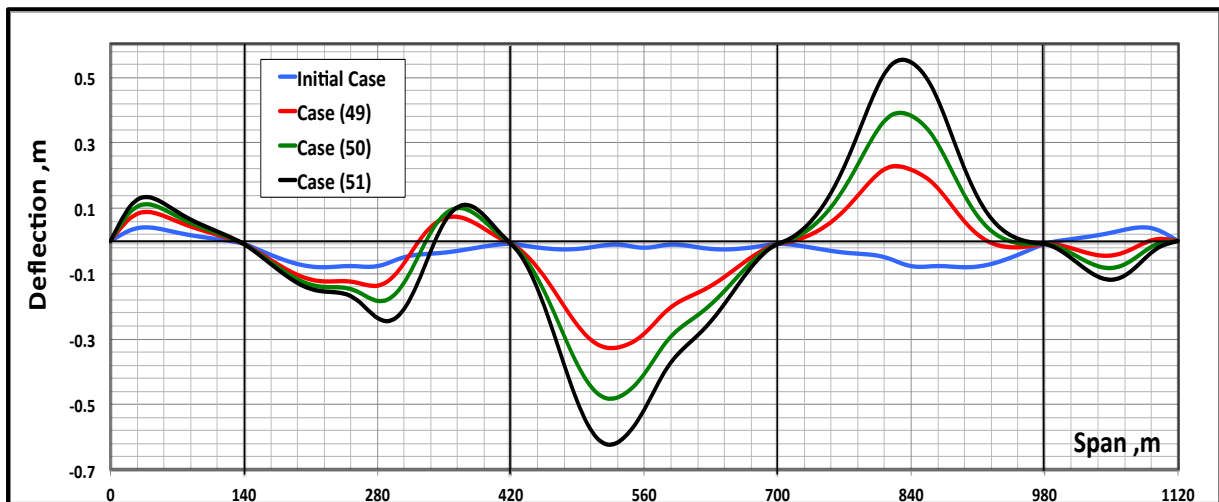


Fig. (12): Vertical deflection of the floor beam (Combination cases)

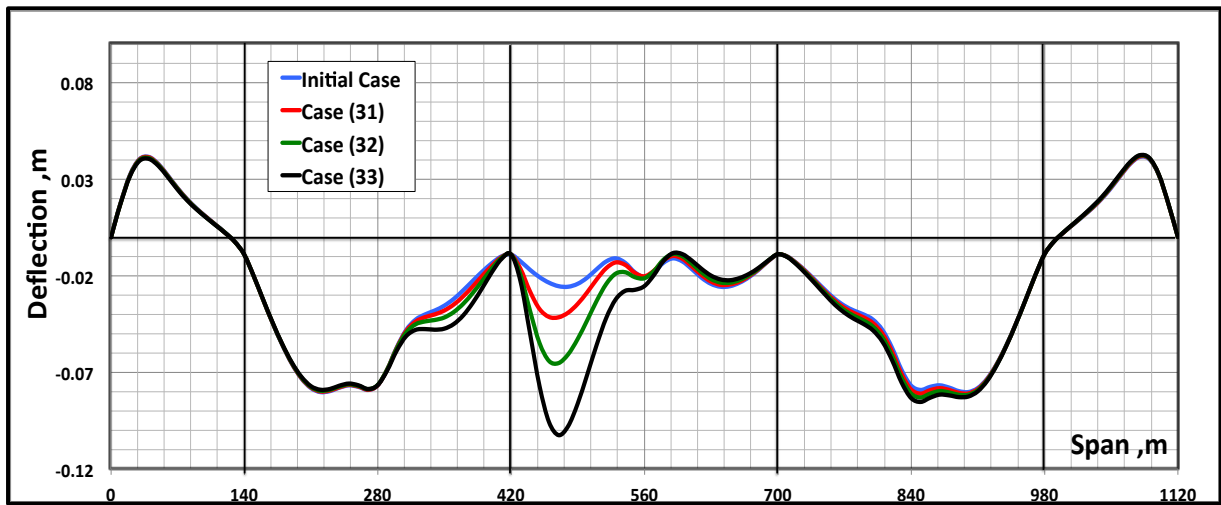


Fig. (13): Vertical deflection of the floor beam (Combination cases)

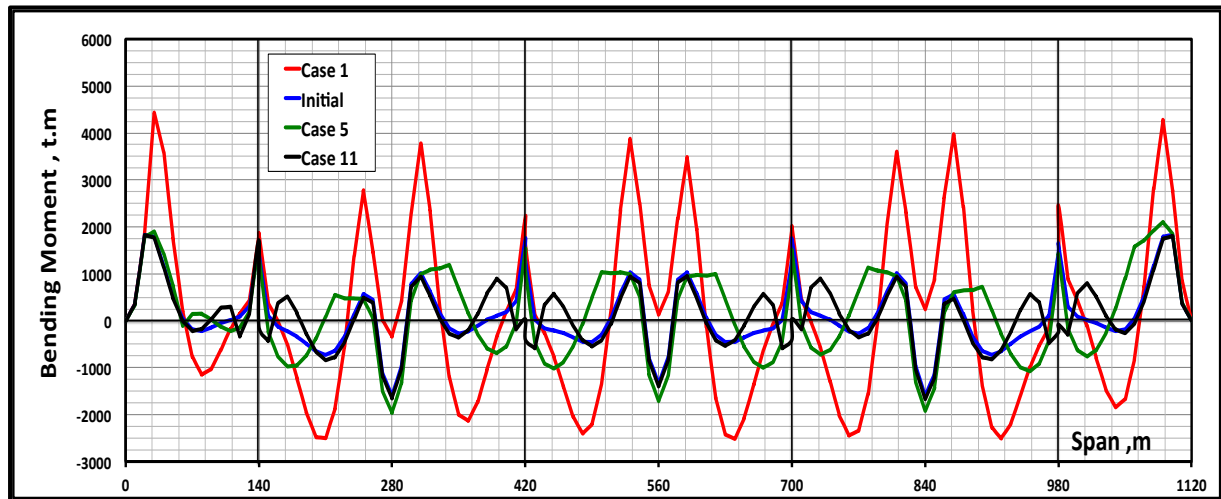


Fig. (14): Bending Moment of the floor beam (Individual cases)

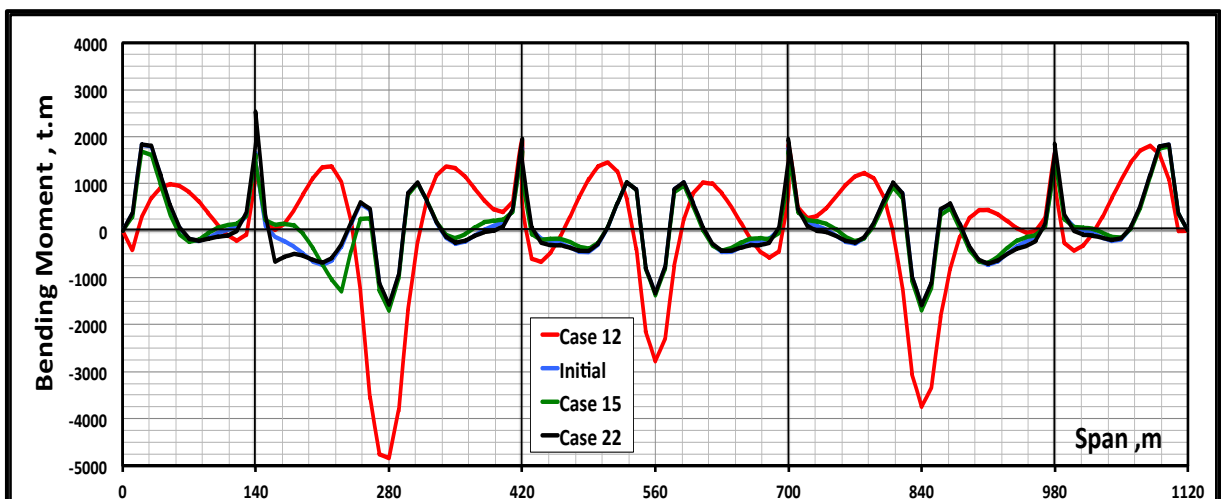


Fig. (15): Bending Moment of the floor beam (individual cases)

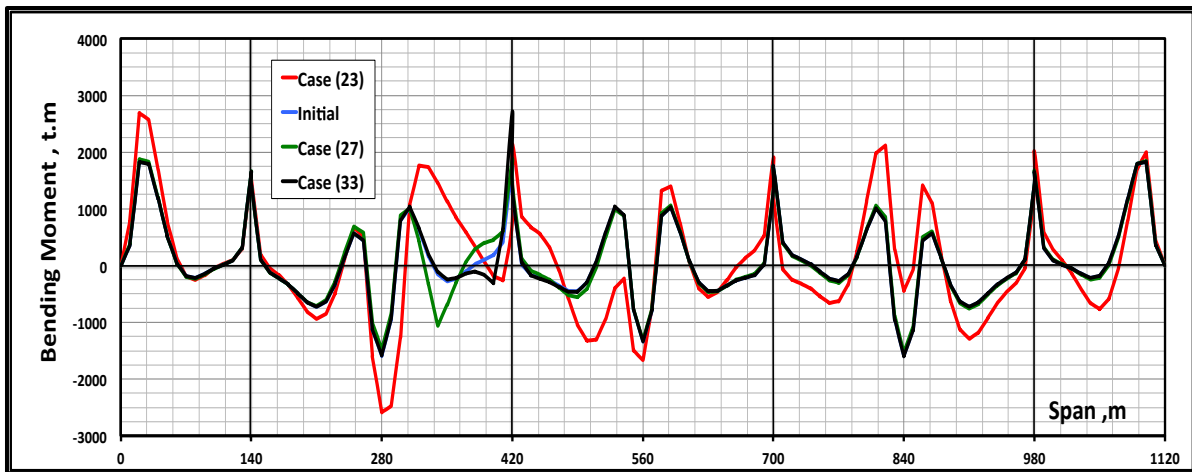


Fig. (16): Bending Moment of the floor beam (individual cases)

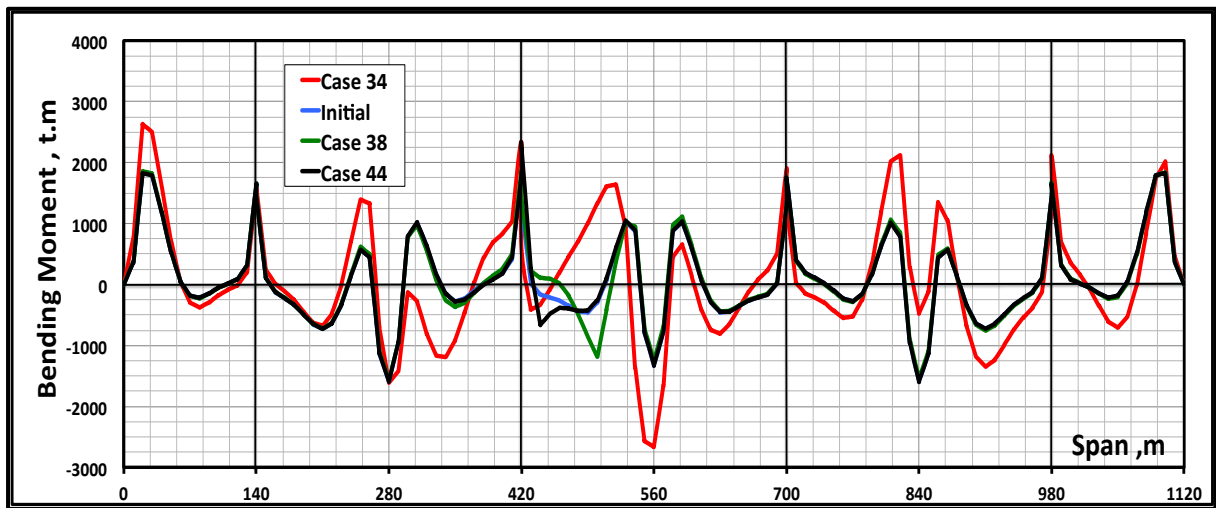


Fig. (17): Bending Moment of the floor beam (individual cases)

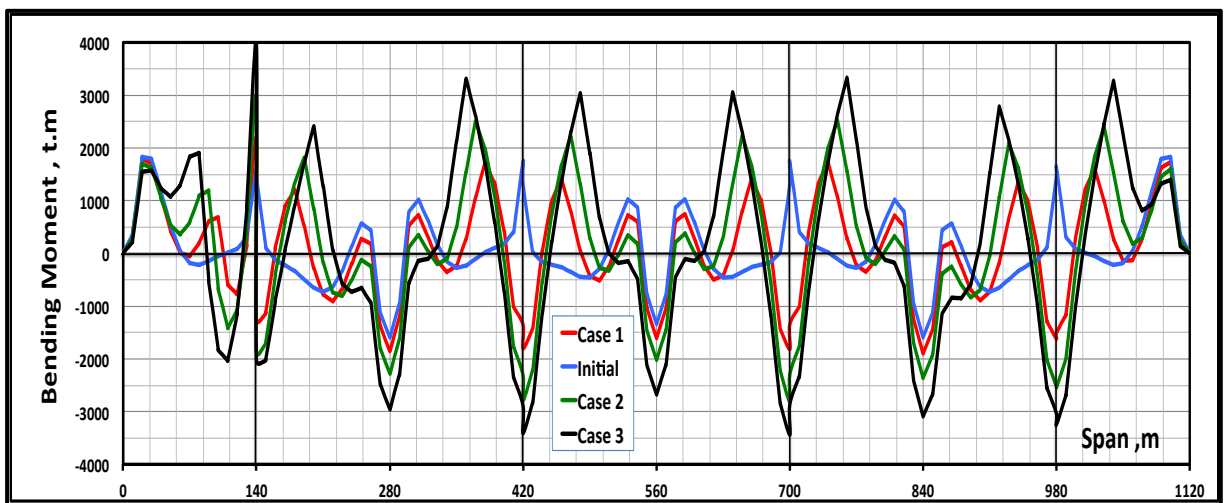


Fig. (18): Bending Moment of the floor beam (Combination cases)

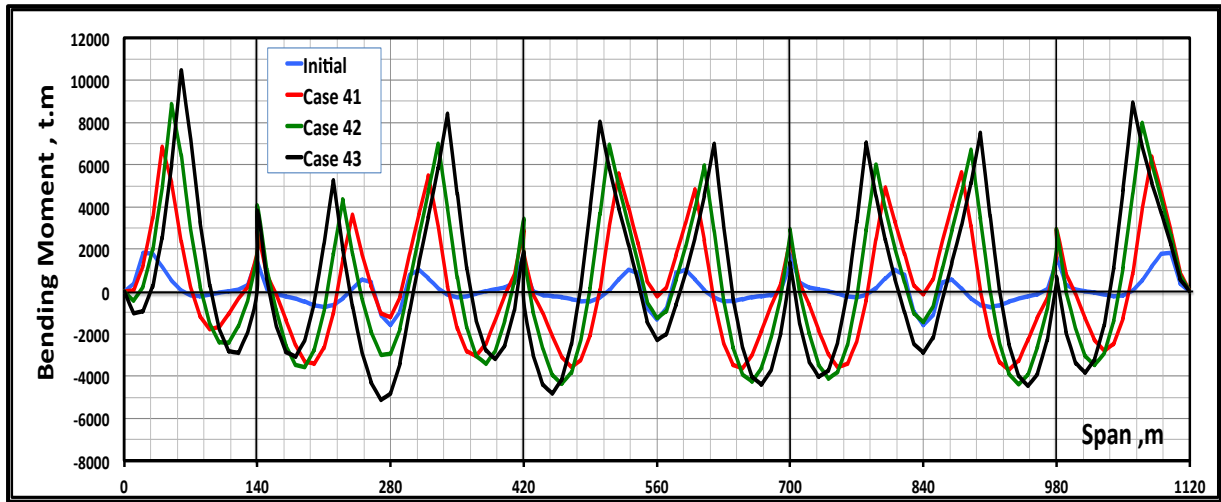


Fig. (19): Bending Moment of the floor beam (Combination cases)

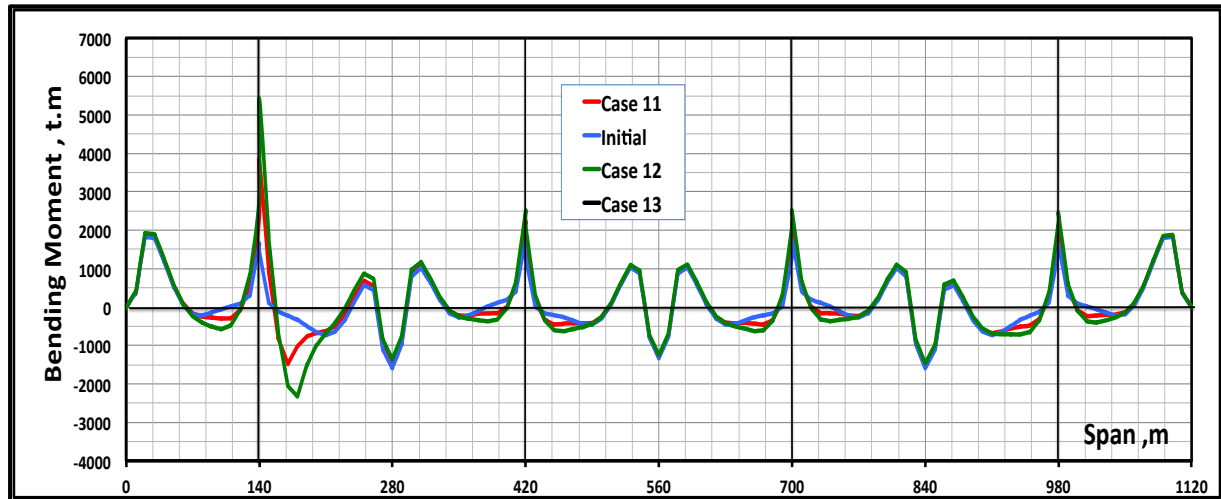


Fig. (20): Bending Moment of the floor beam (Combination cases)

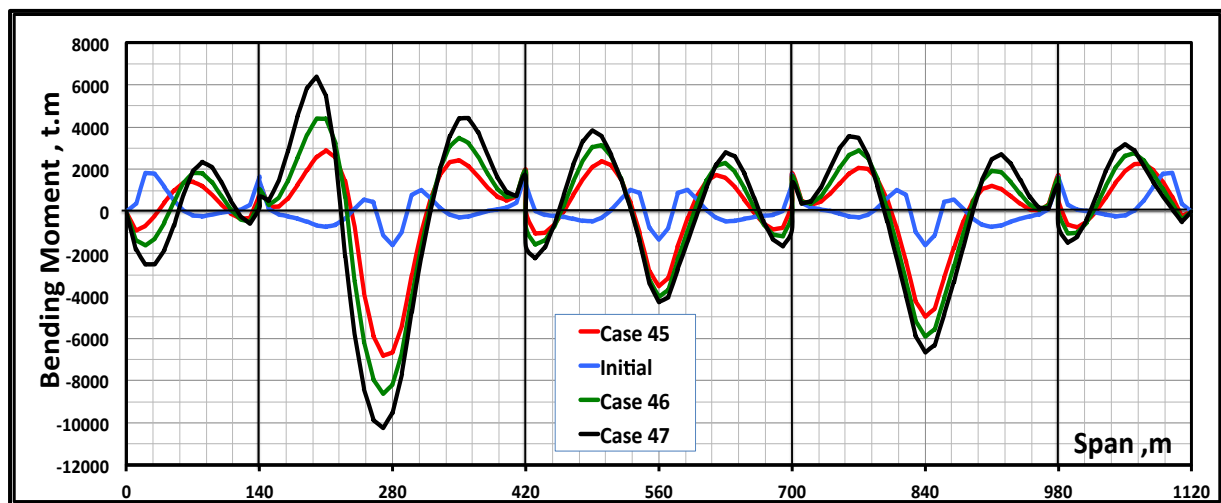


Fig. (21): Bending Moment of the floor beam (Combination cases)

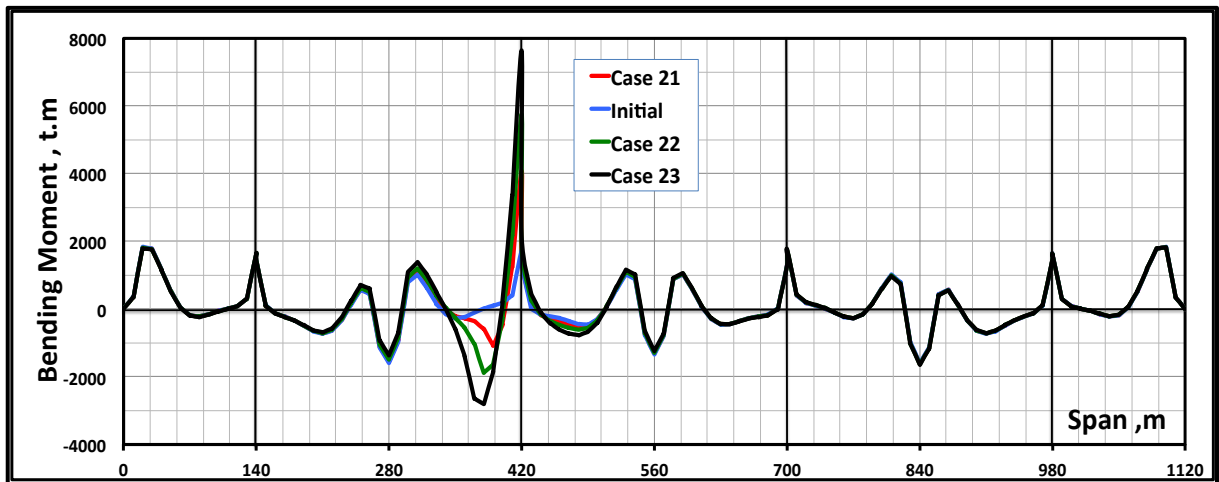


Fig. (22): Bending Moment of the floor beam (Combination cases)

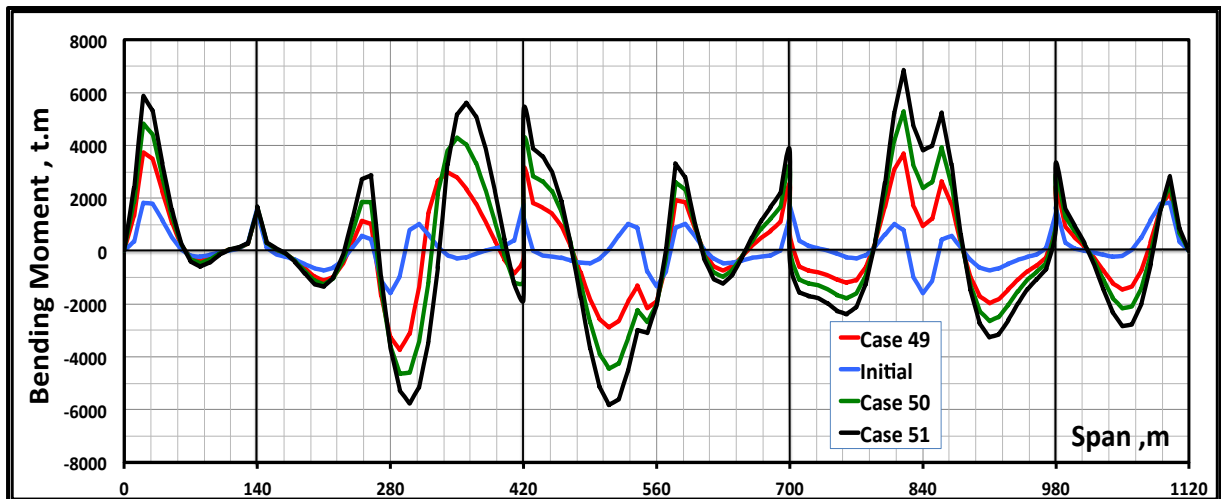


Fig. (23): Bending Moment of the floor beam (Combination cases)

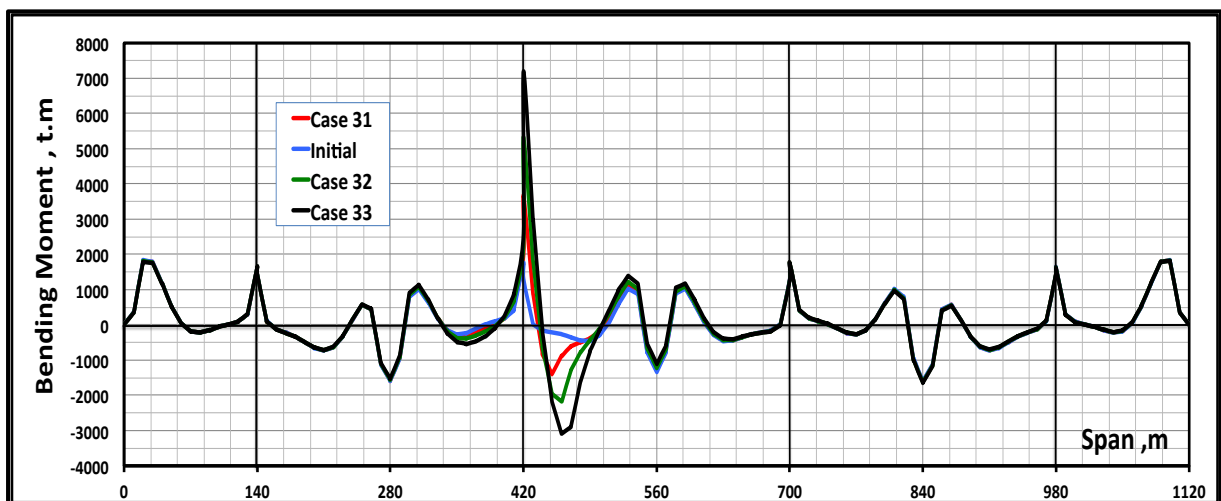


Fig. (24): Bending Moment of the floor beam (Combination cases)

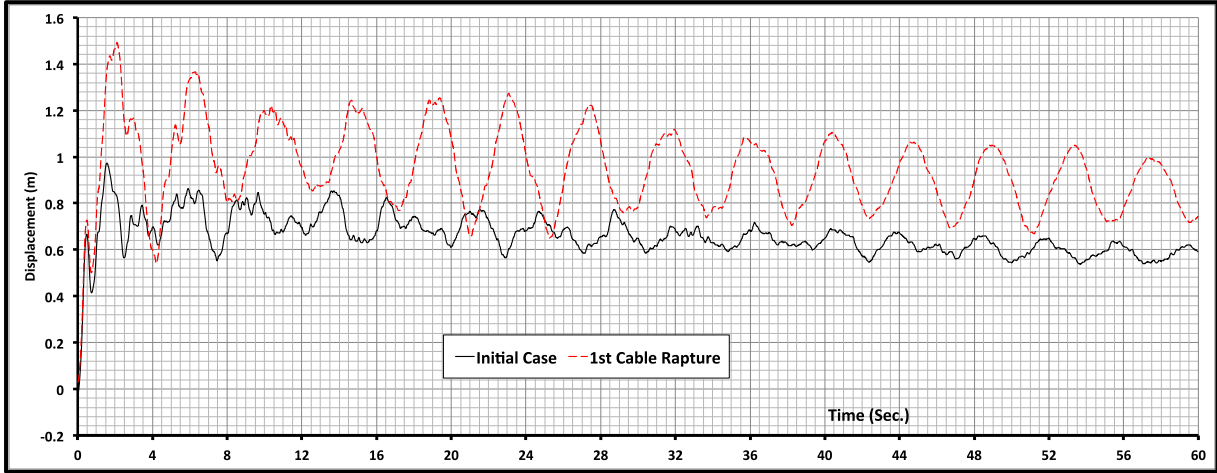


Fig. (25): Displacement of the mid-joint at the 2nd span

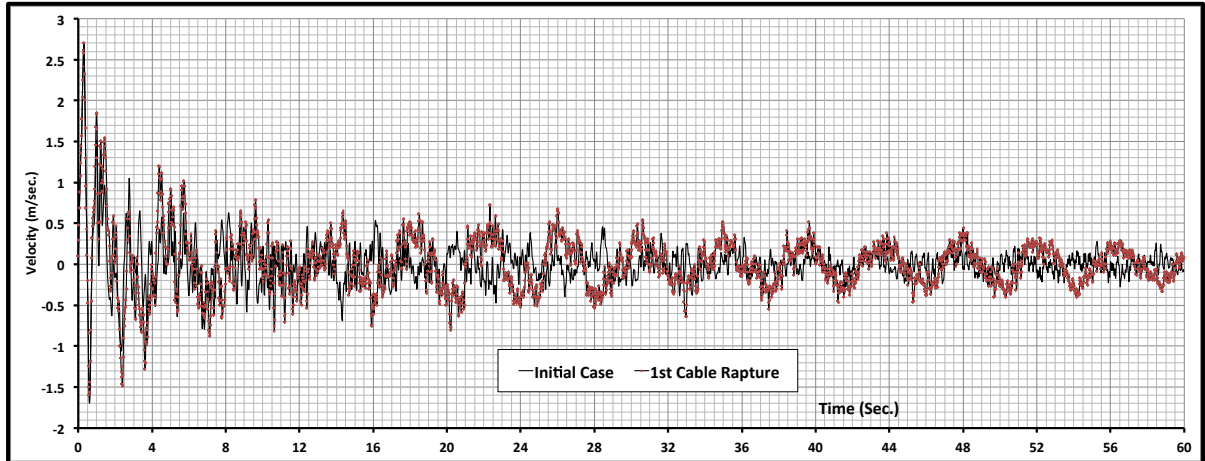


Fig. (26): Velocity of the mid-joint at the 2nd span

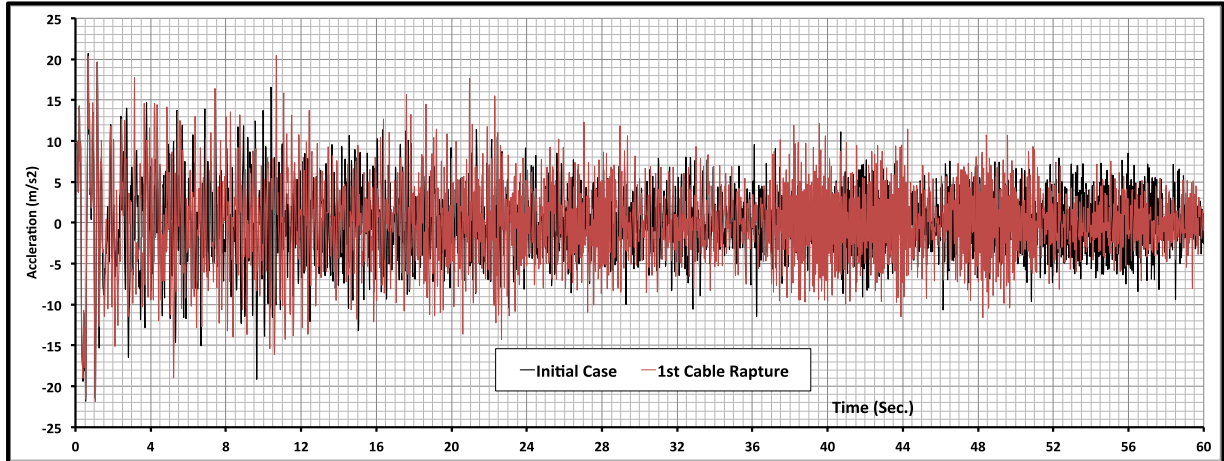


Fig. (27): Acceleration of the mid-joint at the 2nd span

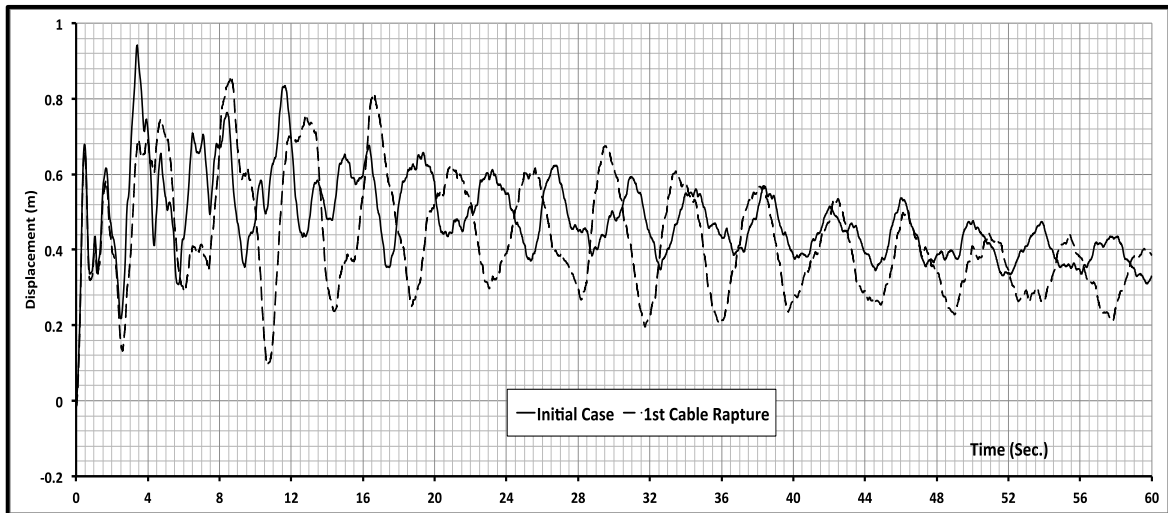


Fig. (28): Displacement of the mid-joint at the 3rd span

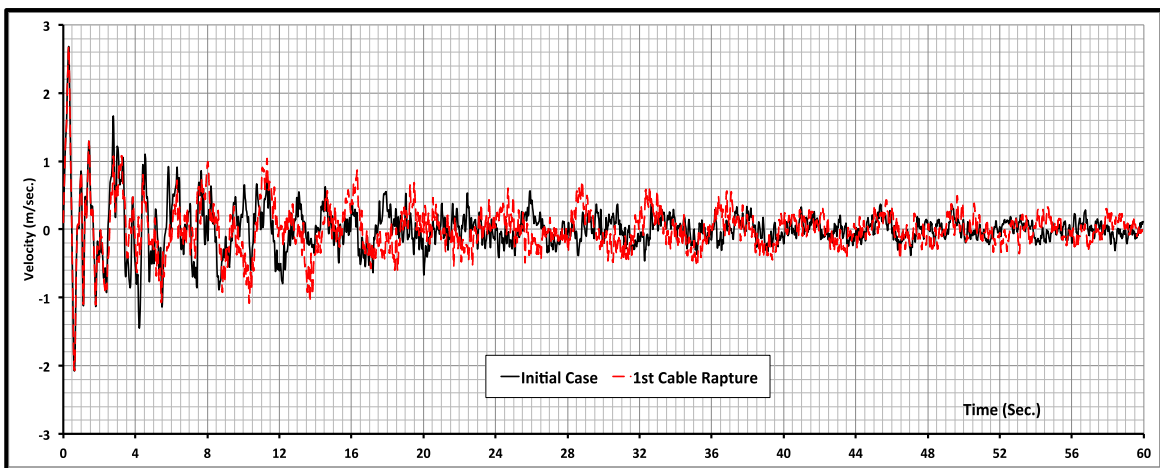


Fig. (29): Velocity of the mid-joint at the 3rd span

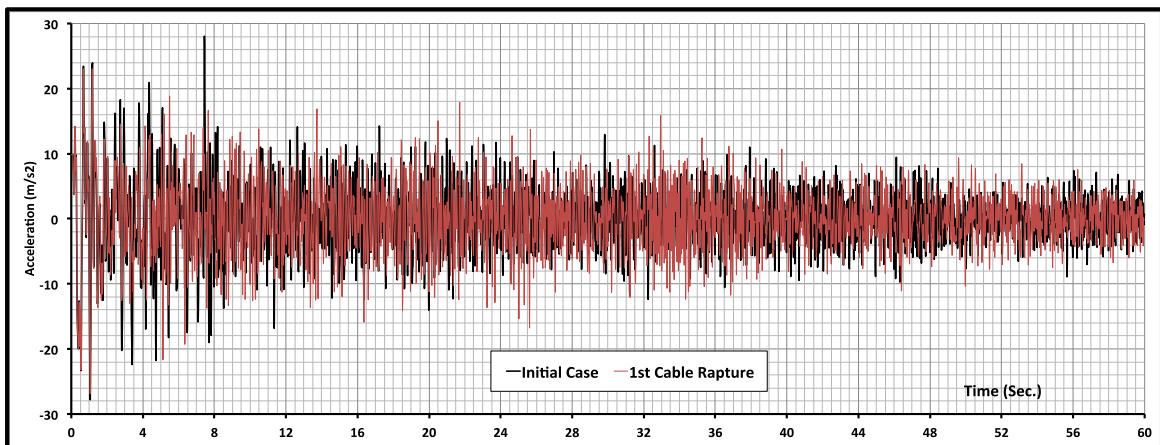


Fig. (30): Acceleration of the mid-joint at the 3rd span

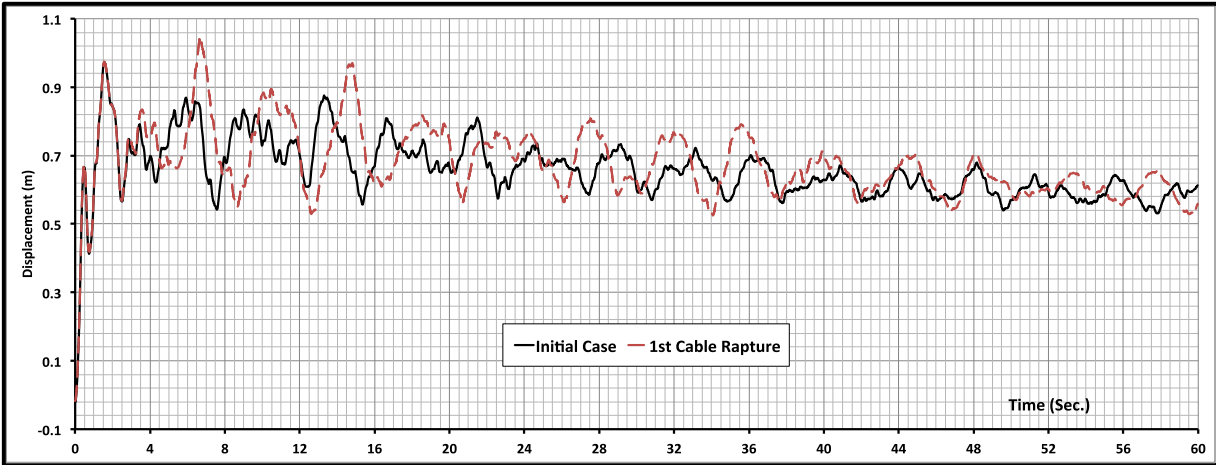


Fig. (31): Displacement of the mid-joint at the 4th span

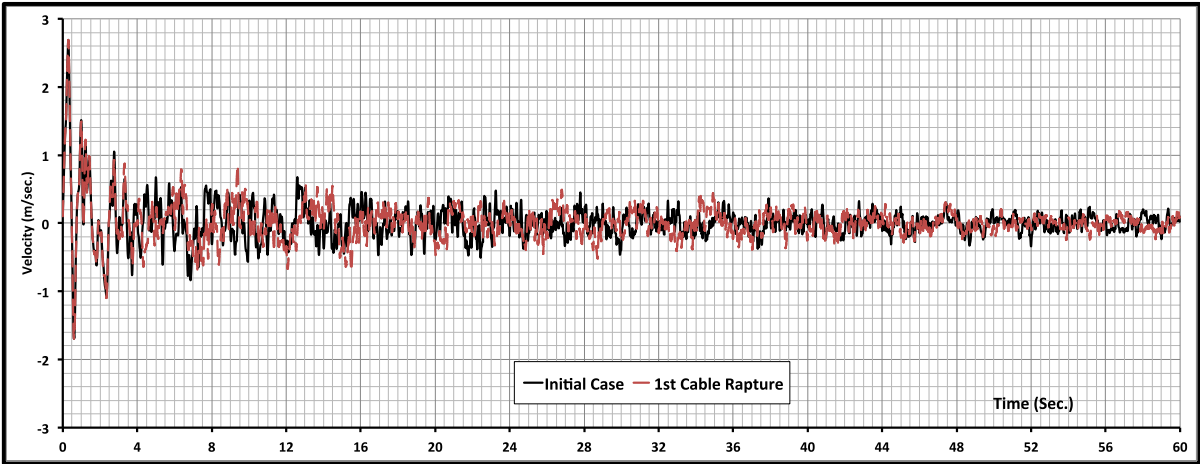


Fig. (32): Velocity of the mid-joint at the 4th span

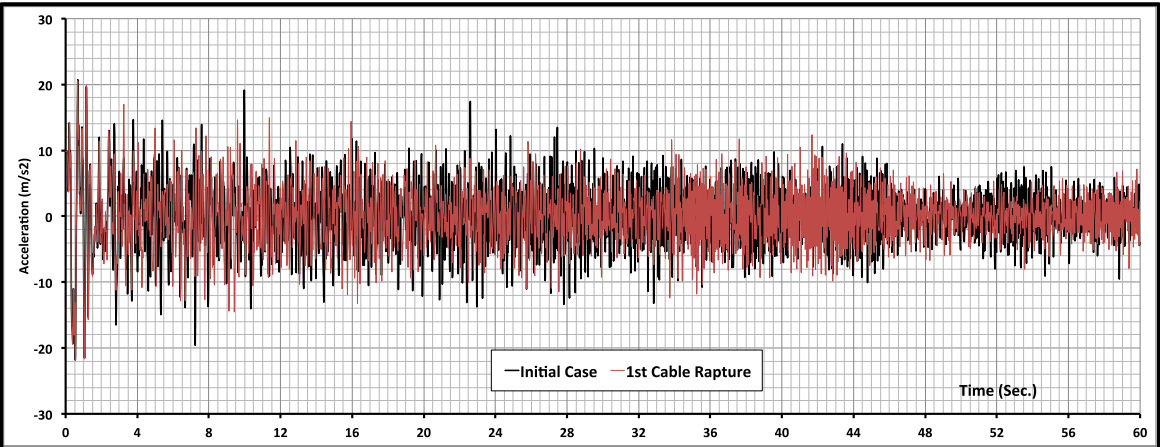


Fig. (33): Acceleration of the mid-joint at the 4th span

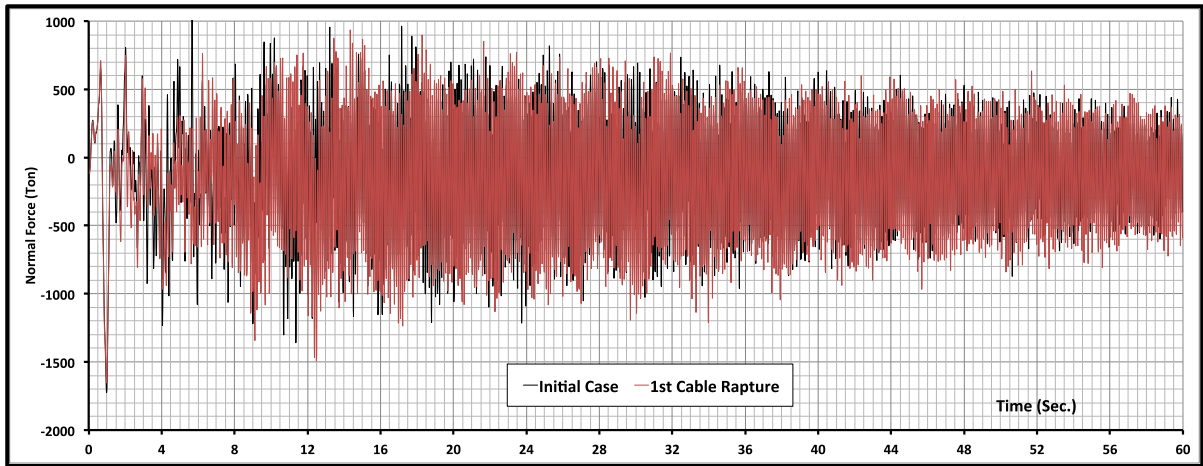


Fig. (34): Normal Force of the mid-joint at the 2nd span

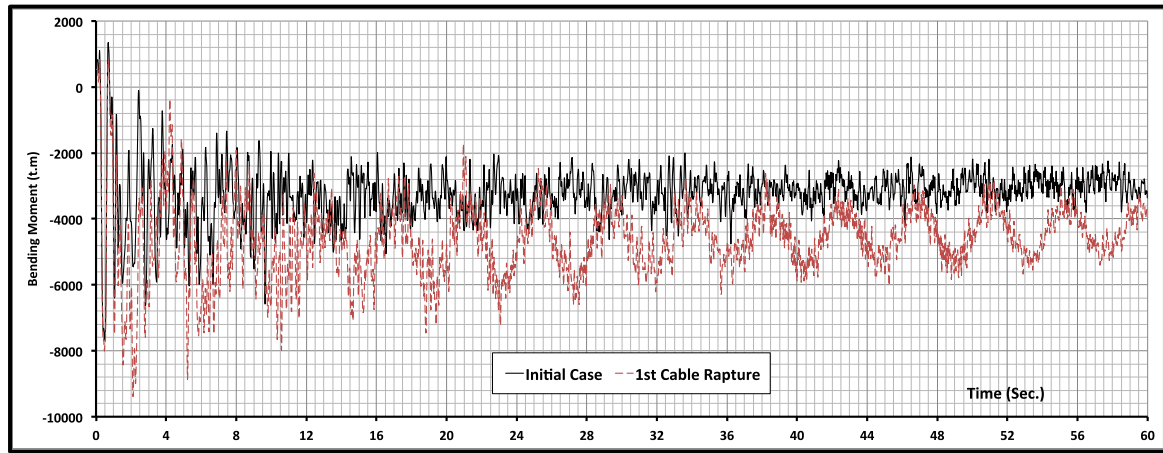


Fig. (35): Bending Moment of the mid-joint at the 2nd span

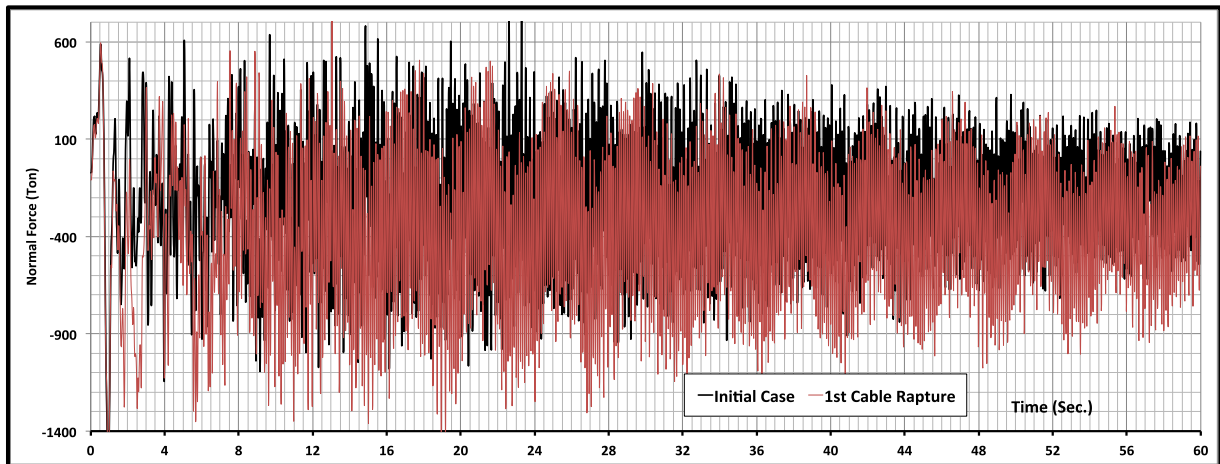


Fig. (36): Normal Force of the mid-joint at the 3rd span

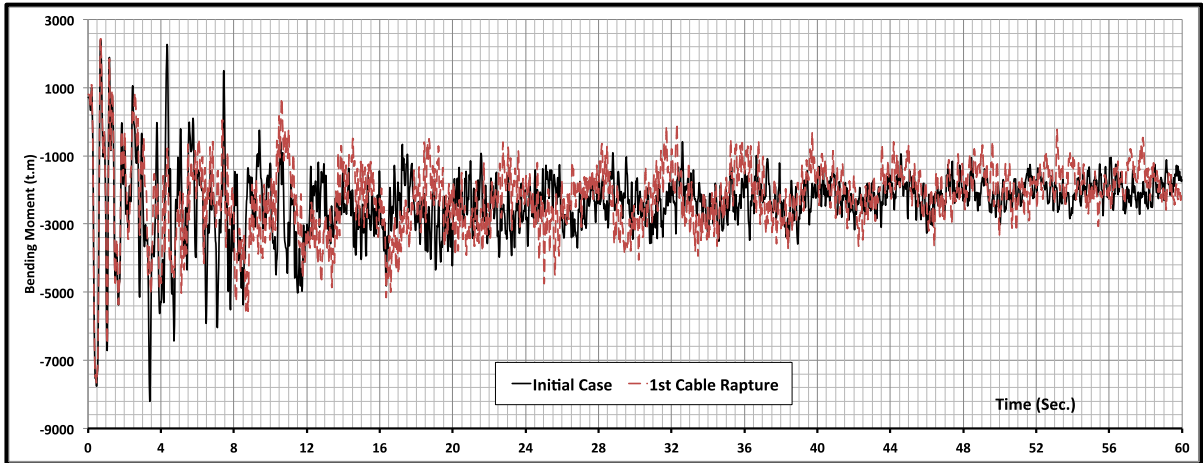


Fig. (37): Bending Moment of the mid-joint at the 3rd span

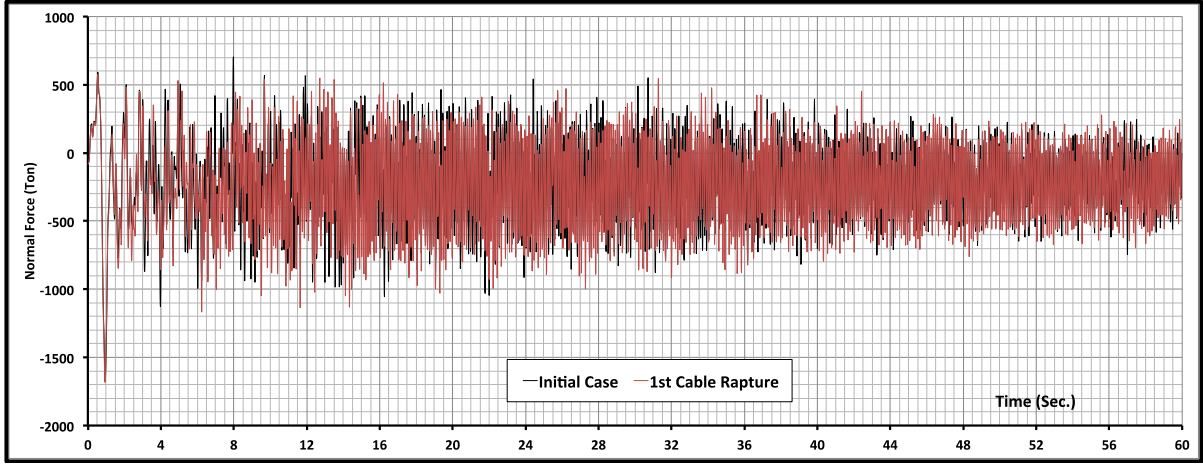


Fig. (38): Normal Force of the mid-joint at the 4th span

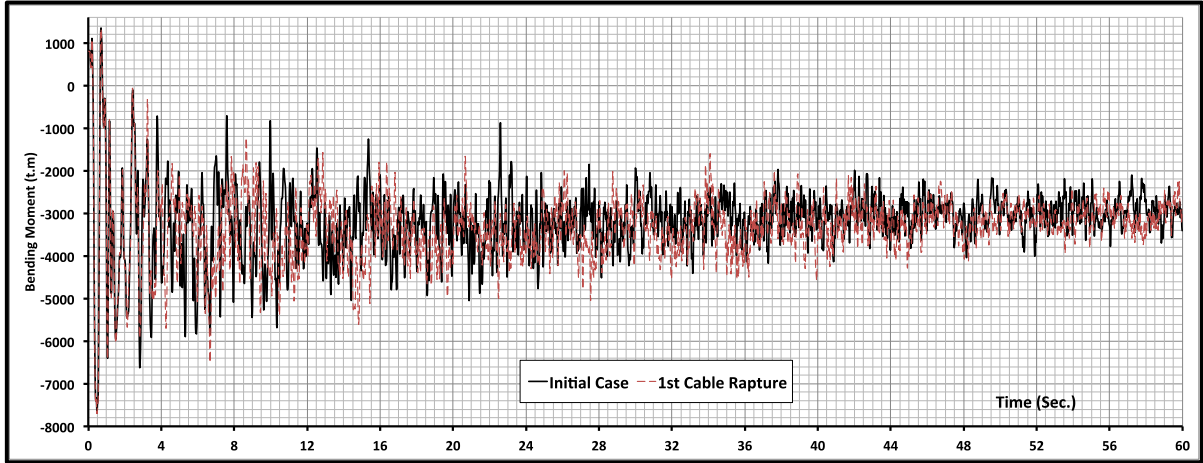


Fig. (39): Bending Moment of the mid-joint at the 4th span